

Laser ablation of organic polymers: Microscopic models for photochemical and thermal processes

Barbara J. Garrison^{a)}

Department of Chemistry, The Pennsylvania State University, University Park, Pennsylvania 16802

R. Srinivasan

IBM Thomas J. Watson Research Center, Yorktown Heights, New York 10598

(Received 1 October 1984; accepted for publication 26 November 1984)

Irradiation of organic polymers by short pulses of far-UV (e.g., 193 nm) laser light causes ablative photodecomposition (APD) of the material. This etching process occurs cleanly leaving behind a well-defined pit. Longer wavelength (e.g., 532 nm) laser light also ablates material from a polymeric solid. However, this process is distinct from APD in that the sample near the pit is distorted and melted. Microscopic models are presented here for both the photochemical and thermal processes. The photochemical model predicts that well-defined pits will be formed, that narrow angular distributions of the ablated material should be observed, and that the average perpendicular ejection velocity will be 1000–2000 m/s. The thermal model predicts melting or distortion of the solid and a broad angular distribution of the ejected material.

I. INTRODUCTION

There has been considerable interest recently in the use of laser radiation to remove material from a solid. Of particular interest is the observation that short pulses of far-UV (e.g., 193 nm) radiation ablates organic material cleanly, i.e., the remaining sample exhibits a precisely defined pit.^{1–12} It is possible that the radiation could have melted or damaged the remaining sample. Indeed for longer wavelength radiation, e.g., visible or infrared light, damaged samples are generally observed.⁹ These differences in pit characteristics are shown in Fig. 1 where cross sections of an aortal wall from a cadaver have been exposed to 193 nm laser light from an ArF excimer laser and to 532 nm or green laser light from a Nd:YAG laser. In the first case the remaining pit is cleanly etched. This process has been called ablative photodecomposition (APD).^{1–3} In the latter case the sample has distorted pit walls and exhibits dehydration, charring, and possibly melting. The discovery that the far-UV radiation can cleanly etch polymeric and biological materials has expanded the possible uses of excimer lasers into such diverse fields as dry etching of photoresists,^{1,7,8} removal of corneal tissue⁵ and ablation of atherosclerotic lesions.⁹

Obviously there are at least two distinct processes that can result in ablation of material when it is irradiated by laser light. In the following discussion we will refer to the phenomenon that cleanly etches the material as the photochemical process and the one that melts the sample as well as etching it as the thermal process. Although from Fig. 1 the two extremes are apparent it is unknown at this time that if the laser wavelength were continuously varied from 192 to 532 nm whether the change in pit characteristics would be continuous or abrupt. Likewise, the precise wavelength regimes appropriate for the photochemical and thermal processes for individual materials are not known.

In order to understand the two ablation processes, the nature of the interaction of the laser radiation with organic materials is examined. The absorption of UV radiation by organic molecules is known to involve an electronic transition to a higher state. This is shown schematically in Fig. 2. Several processes could then occur. If the transition leads to a level above the dissociation limit, then the molecule can dissociate almost immediately. There may also be a curve crossing to a repulsive state which again leads to dissociation. Finally an intersystem crossing can occur, by which the molecule ends up in the ground state. In the first two cases one photon of radiation leads to a bond dissociation and chemical reaction. In the latter case, although it is energeti-



FIG. 1. Cross section of the luminal side of an aortal wall. (Taken with permission from Ref. 9.) (a) 0.35-mm trench produced by far-UV (193 nm) radiation. A Lambda Physik EMG102 argon fluoride laser operating at a wavelength of 193 nm and pulse duration of 14 ns was used. A total of 1000 pulses of fluence 2.5 mJ/mm² was applied to the sample. Approximately 2.5 J/mm² of energy was thus deposited. (b) 0.4-mm crater produced by visible (532 nm) radiation. A Quanta-Ray DCR Nd:YAG laser operating at a wavelength of 532 nm and pulse duration of 5 ns was used. A total of 1800 pulses of fluence 10 mJ/mm² was applied to the sample. Approximately 18 J/mm² of energy was thus deposited.

^{a)} Alfred P. Sloan Research Fellow; Camille and Henry Dreyfus Teacher-Scholar.

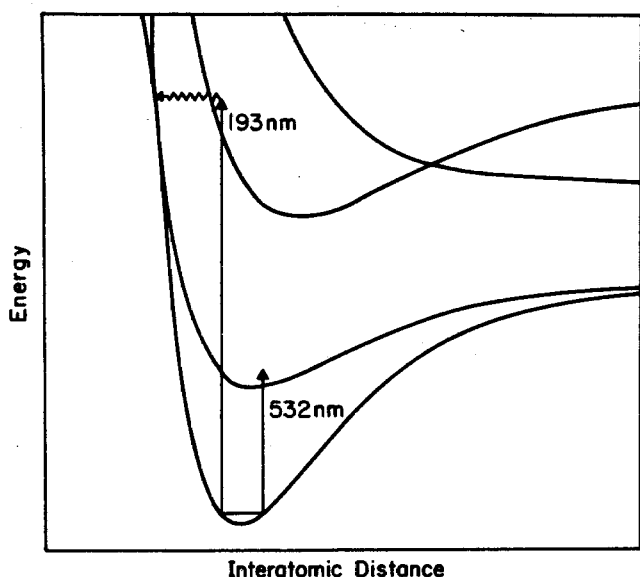


FIG. 2. Schematic potential curves. Indicated on them are typical transitions for various wavelengths of radiation.

cally possible for the molecule to dissociate, much of the energy will be converted to heat and no reaction will occur. Here then are two possible outcomes that can occur when UV photons are used to irradiate an organic molecule. Either a single photon efficiently dissociates the bond or the energy is deposited as heat.

Visible or infrared radiation can also ablate material from a solid. In this case, there is insufficient energy in one photon to break a chemical bond (Fig. 2). Consequently the longer wavelength light is absorbed into the vibrational modes of the molecule either directly or indirectly *via* a low lying electronic state. This is basically a heating process. Eventually one bond may absorb a sufficient number of photons to initiate dissociation. However, during the time it is accumulating sufficient energy to be able to dissociate and desorb, other parts of the sample are absorbing energy by vibrational energy transfer and are thus susceptible to diffusion and melting.

The questions that still remain, however, are (1) how, after the photochemical bond breakage, to explain the ablation of the material from the sample and (2) why does the photochemical process cleanly etch materials while the thermal process melts and damages the sample. In this study we present two microscopic models based on the above physical pictures, one to describe the photochemical process and one for the thermal process. Each model makes specific predictions regarding the experimental observables such as the pit shape, the angular distribution, and the energy distribution of the ablated material.

II. PHOTOCHEMICAL MODEL

The polymer is described by structureless monomer units held together by strong attractive interactions.¹³ After the laser light strikes the sample a few of the monomer units react photochemically. We simulate this process by allowing each monomer unit to undergo excitation directly from an attractive to a repulsive potential surface (i.e., repulsive

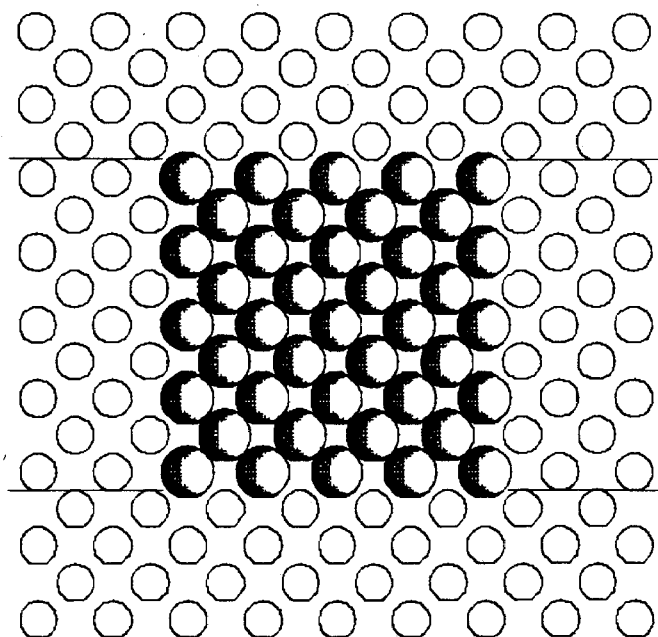


FIG. 3. Surface layer of the ensemble of monomer units. All odd numbered layers have the same configuration of units. The even numbered layers have monomer units in the spaces of the first layer. A total of eight layers is included in the calculations. The radii of the circles are arbitrary although the smaller, plain circles represent the nonirradiated units and the larger, shaded circles the irradiated units. The two horizontal lines show the region of space that is graphically displayed in Figs. 4, 6, and 7.

state). This excitation produces a change in the volume occupied by the monomers. For computational simplicity we assume that the polymer is arranged in a face-centered cubic (fcc) crystalline array. This assumption should not significantly affect the conclusions and makes it visually easier to determine the amount of distortion that occurs. The interaction for the bound monomer units is assumed to be pairwise additive with a Morse form.¹⁴ The repulsive interaction is assumed to have the form $1/r^n$.

A polymer with the characteristics of polymethylmethacrylate (PMMA) was chosen as a model system. This system has a density of 1.22 g/cm^3 .¹⁵ Using the monomer mass of PMMA of 100 amu, this density corresponds to a fcc lattice with a lattice constant of 8.1 \AA . The surface arrangement of monomer units is shown in Fig. 3. We assume that the main attractive forces holding the monomer units together are the two carbon-carbon bonds along the chains. The strength of a C-C bond is approximately 3.6 eV. Given the bond strengths and the distance between the units we can determine the Morse parameters of the corresponding pair potential. In this case they are $D_e = 0.60 \text{ eV}$, $r_e = 5.75 \text{ \AA}$, and $\alpha = 2.0 \text{ \AA}^{-1}$. These parameters yield a cohesive energy for one monomer unit of 3.6 eV. The basic repulsive term is $1/r^{12}$. The coefficient of the $1/r^{12}$ term for the repulsive interaction is chosen to be $6 \times 10^8 \text{ eV \AA}^{12}$ so that the energy of the reacted monomer is 193 nm (6.4 eV) larger than the cohesive energy of the monomer unit in the polymerized form at the same density.

Hamilton's classical equations of motion for the particles are integrated in time. For particle i of mass m_i , the equations are

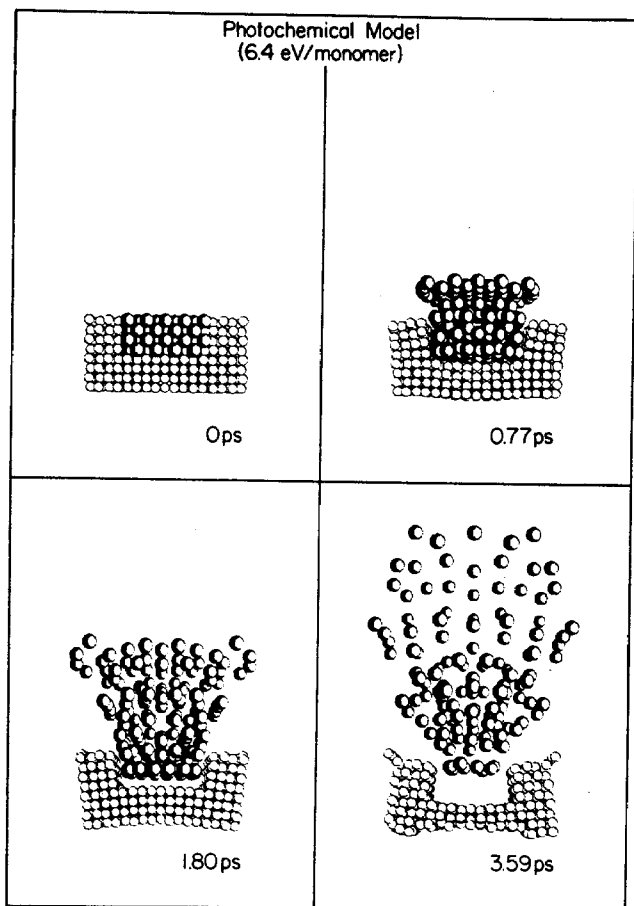


FIG. 4. Photochemical model. Movement of the monomers as a function of time (1 ps = 10^{-12} s). There is a slight perspective in the drawings.

$$m_i \frac{dv_i}{dt} = F_i$$

and

$$\frac{dx_i}{dt} = v_i,$$

where x_i is the position vector, v_i is the velocity vector, and F_i is the force. The coupling between the units is in the force F_i with

$$F_i = -\nabla_i \sum_j V(r_{ij}),$$

where $V(r_{ij})$ is the appropriate pair potential for particles i and j separated by a distance r_{ij} . For N particles there are $6N$ coupled first order differential equations. As initial conditions we assume that the monomers in the central region in the top four layers of the crystal interact *via* the repulsive potential, i.e., they have reacted. In other words, we have assumed that the laser radiation has already been absorbed and the polymer has been fragmented into monomer units. Due to the fcc symmetry this corresponds to 41 monomers in layer 1 and 3 and 40 monomers in layers 2 and 4 for a total of 162 reacted species. Initially the velocities of all the particles are zero. However, since the reacted particles are initially at too high a density, i.e., they interact *via* a repulsive potential, they will gain kinetic energy as time progresses.

Specific predictions regarding the ablation process arise from the calculation.¹³ (i) The reacted material ablates without melting the remainder of the sample. This is shown graphically in Fig. 4 where a time sequence of the nuclear motion is displayed. (ii) The average perpendicular velocity of the ablated material is ~ 1000 – 2000 m/s. As discussed below the precise value depends on the form of the repulsive interaction. (iii) The angular distribution of the ablated material is within $\sim 30^\circ$ of the surface normal (Fig. 5). (iv) The material ablates layer by layer. The sample size used here is not as deep as that used previously.¹³ In addition, the reacted region is larger. This change has been implemented to increase the number of units in the center of the irradiated region relative to the number adjacent to the pit walls.

On built-in assumption in the model is that there is a repulsive interaction among the reacted monomers or new photochemical products and between these new species and the remaining sample, consequently all of the photochemically reacted species will eventually ablate. It is difficult then to determine an excitation or wavelength threshold with this model. As long as the excitation is greater than ~ 3.6 eV ($\lambda < 340$ nm) there will be photochemical ablation, i.e., minimal sample melting. The effect of excitation of a fraction the monomers in the central region is discussed in Ref. 13. The

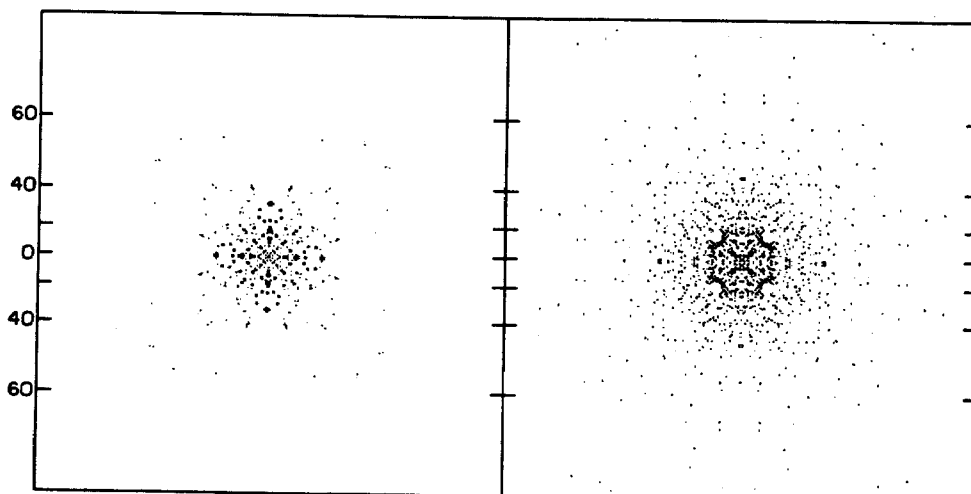


FIG. 5. Angular distribution of the ablated material. Each ejected monomer is plotted on a flat-plate collector an arbitrary distance above the crystal. The radial distance of a plotted point from the center of the plate indicates the polar angle of ejection. The polar angle scale is shown on the left. In both cases the data have been symmetrized to reflect the crystalline solid because a darker visual image results. Photochemical model (left). Thermal model (right). This distribution is from the calculation in which each monomer was given 6.4 eV of kinetic energy. Four different distributions of initial velocities have been calculated so that the total number of ejected particles is the same in both frames.

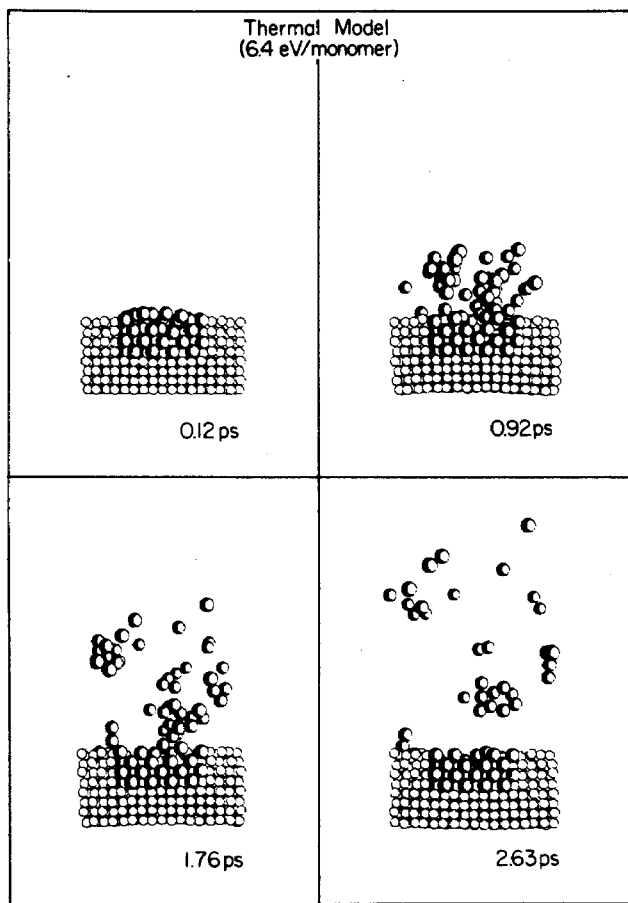


FIG. 6. Thermal model. Initially each irradiated monomer had 6.4 eV of kinetic energy.

form of the repulsive interaction (e.g., $1/r^{15}$, $1/r^{12}$, or $1/r^6$) will influence the final average velocity and the time scale of the ablation, but will not alter the predictions of a clean etch and a narrow angular distribution.

III. THERMAL MODEL

For irradiation of solids by laser frequencies corresponding to energies less than chemical bond strengths (~ 3.6 eV or $\lambda > 340$ nm), it is obvious that one photon is incapable of directly forcing the molecule to undergo an electronic transition such that a bond is broken. Thus it seems plausible that the photon energy excites vibrations within the molecules (i.e., heat). As discussed in the Introduction the vibrational modes may be excited in several ways. The ablation of the material, then, corresponds to an evaporation rather than a volume explosion. For evaporation (or thermal desorption from solids) several quanta of laser energy are required to be localized in one bond so that it may break. During the time that the energy is accumulating in this bond, other regions of the sample are becoming vibrationally excited, and possibly melted.

We model the thermal process by again assuming that we have an fcc crystal of structureless monomer units. In this case only the attractive potential is used. As initial conditions, the irradiated monomers are each given kinetic energy equal to the energy of one photon. As in the photochemical model the laser radiation is assumed to be already absorbed.

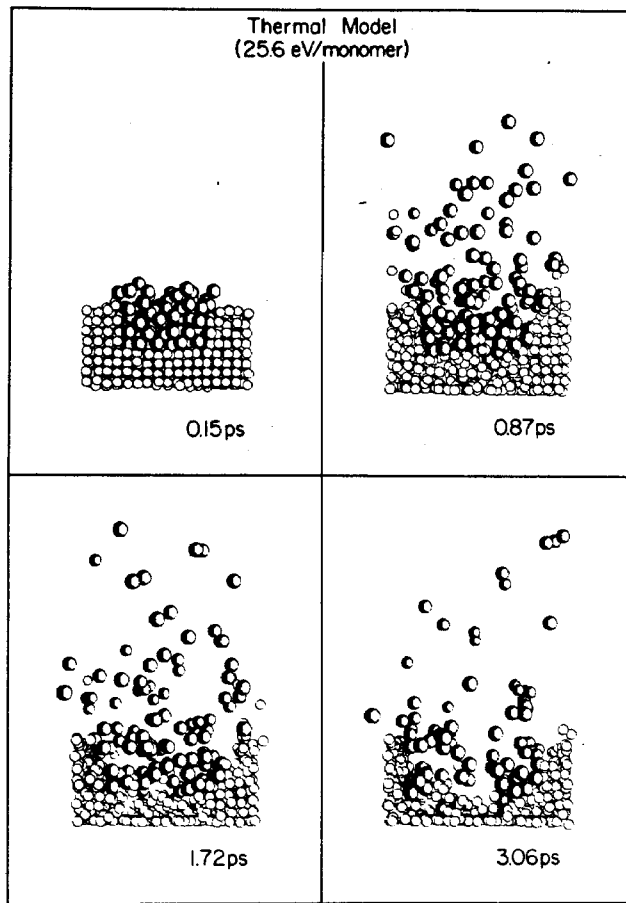


FIG. 7. Thermal model. Initially each irradiated monomer had 25.6 eV of kinetic energy.

In this case the central region of the solid is excited vibrationally but the dissociation into monomers has not occurred. A value of 6.4 eV is used for the kinetic energy of each monomer so that direct comparisons with the photochemical model can be made. The velocity vector of each irradiated unit is randomly oriented. Initially each irradiated monomer has sufficient energy to escape the solid; however, not all the velocity vectors are oriented out of the crystal. In addition, there is a time delay between when monomers in the first layer eject and when those in the deeper layers may reach the surface. During this time collisions between the irradiated or energized units and the surrounding solid occur and energy is transferred to the solid. Some of the energized monomers may lose sufficient energy such that they are trapped in the solid and do not ablate.

A time sequence of monomer positions is shown in Fig. 6 for the thermal model in which each irradiated unit was initially given 6.4 eV (193 nm) of kinetic energy. A total of 162 monomers in four layers was irradiated. Both the photochemical system shown in Fig. 4 and the thermal system shown in Fig. 6 initially had the same amount of total energy. Only $\sim 30\%$ of the monomers eject in the thermal model with the remainder losing sufficient energy to become trapped in the solid. Approximately 75% of the first layer of excited monomers, 30% of the second layer of excited monomers, and virtually none from the third and fourth layers ejected. The small pit which does exist is in the center of the

top two layers and does not show up well in Fig. 6. A few of the irradiated units start to eject but do not have sufficient energy to escape their attraction to the solid and end up migrating along the surface. A similar migration phenomenon has been observed in simulations of keV ion bombardment of solids.¹⁶ The most important conclusion from the calculation is that if each unit only absorbs into vibrational modes *one* photon of 193 nm laser light, a significant pit is *not* formed. This difference in the energy threshold for the two processes has been observed by Linsker *et al.*⁹ For equal amounts of UV and visible energy, only the UV radiation caused complete ablation of the irradiated region.

Whereas one photon per monomer in the photochemical model caused complete ablation, in the thermal model for the same energy input only ~30% of the monomers ejected. In order to obtain a significant amount of ablation in the thermal model we allowed each irradiated unit to absorb two, three, or four photons of energy. The calculation in which the equivalent of four photons of energy (25.6 eV) was given as kinetic energy to each monomer is shown in Fig. 7. Here a larger final pit is obtained. In the process, however, considerable mixing (melting) of the irradiated and nonirradiated monomers has occurred. There is also sputtering of some of the nonirradiated units. Thus we can obtain ablation by this thermal mechanism but it does not result in a cleanly etched pit.

The predicted angular distribution of the ablated material in the thermal model is very broad as is shown in Fig. 5. This is in sharp contrast to the angular distribution from the photochemical model which is narrow. It is difficult to obtain a realistic energy distribution of the ablated material in the thermal model. The energy of the ejected material depends very strongly on the distribution of initial energies that are assigned to the irradiated monomers. One observation is that a few of the ejected species have more kinetic energy than they were given originally. An energetic monomer in the crystal collides with one that eventually ejects, and transfers part of its kinetic energy.

The photochemical model predicts that the material ablates layer by layer. In the thermal model, fragments from the second and third layers ejected while some from the first layer did not. Thus the material does not ablate layer by layer.

IV. COMPARISON WITH EXPERIMENTAL DATA

The most obvious observable to compare with the experimental results is the pit shape of the remaining sample. In the photochemical model the pit is well-defined and cleanly etched (Fig. 4). The thermal model predicts the pit to be rough and exhibit features of melting (Figs. 6 and 7). From the comparison of these results with the two photographs in Fig. 1, it seems apparent that the photochemical mechanism dominates the ablation for the far-ultraviolet laser irradiation of this sample and the thermal mechanism dominates for the visible laser irradiation.

The next observable predicted by both the models is the angular distribution of the ablated material. In the photochemical model the angular distribution is within 25°–30° of the surface normal. The thermal model predicts a broad dis-

tribution out to 60°–70° from the surface normal. Experimental measurements of the angular distribution of the material ablated from polyimide films by 193-nm laser light are consistent with the photochemical model.¹⁷ The angular distribution of material ablated from graphite with a 1.06- μm laser beam of fluence ~1000 J/cm² and pulse width ~1 ns has been measured and found to spread to over 60° from the surface normal.¹⁸ This, then, is consistent with the thermal model.

Unfortunately it is not possible to make reliable estimates of the energy distribution of the ablated material in the thermal model. Depending on the precise choice of parameters in the repulsive potential (i.e., $1/r^n$) in the photochemical model, a value of the average perpendicular velocity is 1000–2000 m/s. This is in excellent agreement with the measurement of Srinivasan and Liu, who found $\langle v_1 \rangle \approx 2200$ m/s for the material ablated from poly(ethylene terephthalate) by 193 nm laser light.¹⁷ A similar ejection velocity has been measured by others.⁶

Predicting the nature of the fragments that are ablated is beyond the scope of either of these models. However, there is a distinct possibility that the dissociation pathways in the two processes are distinct. This appears to be another experimental means of distinguishing between photochemical and thermal ablative decomposition. It should be pointed out that the "monomers" in both of the models represent all the possible fragments that may occur. There may well be monomers ablated¹⁹ but there may also be smaller molecules² and possibly even larger species.²⁰

V. CONCLUSION

Microscopic models for photochemical and thermal ablation of polymer films due to pulsed laser radiation are presented. The photochemical model is appropriate for UV (e.g., 193 nm) radiation and assumes that the laser light initiates a chemical reaction. The products have a larger specific volume than the original sample and an explosion occurs. The predictions of the photochemical model are as follows: (1) The reacted material ablates without melting the remainder of the sample. (2) The average perpendicular velocity of the ablated material is 1000–2000 m/s. (3) The angular spread is within 25°–30° of normal and peaked in the direction normal to the surface. (4) The material ablates layer by layer.

The thermal model assumes that the laser radiation is absorbed into the vibrational modes of the solid. The net effect is a localized heating of the solid resulting in evaporation. This model is applicable for irradiation of the solid by laser light of insufficient energy to photochemically dissociate chemical bonds and possibly even cases of UV irradiation of solids. The predictions of the thermal model are as follows: (1) The remaining sample is distorted and melted. (2) The angular spread is twice as large as that from the photochemical model. (3) The material does not necessarily ablate layer by layer.

The precise wavelength regime in which the photochemical, thermal, or possibly even both processes are operative will undoubtedly depend on the characteristics of individual materials. It is time to make systematic experimental studies

in order to quantitatively define these two regimes and to understand their similarities and differences.

ACKNOWLEDGMENTS

Partial support for these studies is gratefully acknowledged from the Office of Naval Research and the National Science Foundation. One of us (B.J.G.) also thanks the Alfred P. Sloan Foundation for a research fellowship and the Camille and Henry Dreyfus Foundation for a grant for newly appointed young faculty.

¹R. Srinivasan and V. Mayne-Banton, *Appl. Phys. Lett.* **41**, 576 (1982).

²R. Srinivasan and W. J. Leigh, *J. Am. Chem. Soc.* **104**, 6784 (1982).

³R. Srinivasan, *J. Vac. Sci. Technol. B* **1**, 923 (1983).

⁴J. E. Andrew, P. E. Dyer, D. Forster, and P. H. Keys, *Appl. Phys. Lett.* **43**, 717 (1983).

⁵S. L. Trokel, R. Srinivasan, and B. Braren, *Am. J. Ophthalmol.* **96**, 710 (1983).

⁶G. Koren and J. T. C. Yeh, *Appl. Phys. Lett.* **44**, 1112 (1984).

⁷M. W. Geis, J. N. Randall, T. F. Deutsch, P. D. Graff, K. E. Krohn, and L. A. Stern, *Appl. Phys. Lett.* **43**, 74 (1983).

⁸T. F. Deutsch and M. W. Geis, *J. Appl. Phys.* **54**, 7201 (1983).

⁹R. Linsker, R. Srinivasan, J. J. Wynne, and D. R. Alonso, *Lasers in Surgery and Medicine*, **4**, 201 (1984).

¹⁰R. Srinivasan and B. Braren, *J. Polym. Sci., Polym. Chem. Ed.* **22**, 2601 (1984).

¹¹P. E. Dyer and J. Sidhu, *J. Appl. Phys.* **57**, 1420 (1985).

¹²G. M. Davis, M. C. Gower, C. Fotakis, T. Efthimiopoulos, and P. Argyrakis, *Appl. Phys.* (in press).

¹³B. J. Garrison and R. Srinivasan, *Appl. Phys. Lett.* **44**, 849 (1984).

¹⁴H. Eyring, J. Walter, and G. E. Kimball, *Quantum Chemistry* (Wiley, New York, 1944), p. 272.

¹⁵*Encyclopedia of Polymer Science and Technology* (Interscience, New York, 1964), Vol. 4, p. 476; Vol. 3, p. 840.

¹⁶D. E. Harrison, Jr., P. W. Kelly, B. J. Garrison, and N. Winograd, *Surf. Sci.* **76**, 311 (1978); B. J. Garrison and N. Winograd, *Science* **216**, 805 (1982).

¹⁷R. Srinivasan and S. -H. Liu (unpublished).

¹⁸M. A. Covington, G. N. Liu, and K. A. Lincoln, *AIAA J.* **15**, 1174 (1977).

¹⁹R. Srinivasan and S. Lazare, *Polymer* (in press).

²⁰H. H. G. Jellinek and R. Srinivasan, *J. Phys. Chem.* **88**, 3048 (1984).